Journal of Power Sources 189 (2009) 909–915

Contents lists available at ScienceDirect

Journal of Power Sources

journal homepage: www.elsevier.com/locate/jpowsour

Synthesis of carbon-supported Pd-Sn catalyst by ultrasonic irradiation for oxygen reduction reaction

Jandee Kim[a], Toshiyuki Momma[b], Tetsuya Osaka[a,*]

[a] Majored in Applied Chemistry, Graduate School of Advanced Science and Engineering, Waseda University, 3-4-1 Okubo, Shinjuku-ku, Tokyo 169-8555, Japan
[b] Waseda Institute for Advanced Study, Waseda University, 1-6-1 Nishi-Waseda, Shinjuku-ku, Tokyo 169-8050, Japan

ARTICLE INFO

Article history:
Received 21 October 2008
Received in revised form 12 December 2008
Accepted 23 December 2008
Available online 31 December 2008

Keywords:
Oxygen reduction catalysts
Non-Pt catalyst
Ultrasound
Methanol fuel cell
Alkaline media

ABSTRACT

Carbon-supported Pd-Sn (Pd-Sn/C) catalyst was prepared under ultrasonic irradiation, and its electrocatalytic activity for oxygen reduction reaction (ORR) was evaluated in 0.5 M KOH. TEM images showed that the prepared Pd-Sn/C catalyst particles are smaller in average size than carbon-supported Pd (Pd/C) catalyst particles. XRD and XPS results indicated the small particle size and the electronic interaction between Pd and Sn for the Pd-Sn/C catalyst. The Pd-Sn/C catalyst has a higher ORR activity than the Pd/C catalyst in alkaline media. In addition, the Pd-Sn/C catalyst showed a lower Tafel slope and a larger number of electrons transferred for ORR, compared with those of the Pd/C catalyst. These results indicate that Sn influences both the kinetics and the mechanism of ORR. Based on these results, the Pd-Sn/C catalyst prepared by using ultrasonic irradiation can be expected as a promising ORR catalyst in alkaline media.

1. Introduction

Direct methanol fuel cell (DMFC) has been attracting attention as a promising alternative energy source because of the high theoretical energy density and the advantage of using the liquid fuel [1,2]. However, currently available DMFC systems suffer from technical problems such as a low electrocatalytic activity and the methanol crossover, which means the permeation of methanol from the anode side to the cathode side of the cell through the electrolyte membrane [3]. Moreover, platinum metal, which is widely used as the electrocatalyst in DMFC, is expensive, and its limited supply poses a serious problem in commercialization of fuel cell technology [4]. Accordingly, the cathode catalyst of DMFC requires a high activity for oxygen reduction, methanol tolerance and a low cost.

Many studies have been carried out to reduce the loading of Pt by increasing the utilization efficiency of Pt and/or to replace it with a less expensive material [5–7]. Especially, platinum-free catalysts for oxygen reduction reaction (ORR), such as non-platinum metals combinations, metal oxides, chalcogenides, inorganic and organometallic complexes, have been studied [8–14]. Though they generally exhibit a lower catalytic activity, recent studies on Pd-based electrocatalysts show that they have remarkable activities for oxygen reduction. Bard et al. reported that palladium-based electrocatalysts such as Pd–Co–Au (Pd:Co:Au = 70:20:10 atom%), Pd–Ti (Pd:Ti = 50:50 atom%), and Pd–Co–Mo (Pd:Co:Mo = 70:20:10 atom%) which were synthesized by the conventional borohydride reduction method and the reverse microemulsion method, show a reasonable catalytic activity comparable to that of Pt for ORR in PEMFC at 60 °C [15–17]. Ota et al. reported that palladium-based alloys such as Pd–Co, Pd–Ni, and Pd–Cr, prepared by rf sputtering, showed a higher ORR electrocatalytic activity than Pd in sulfuric acid solution, although it was lower than Pt. Those Pd alloys had no electrocatalytic activity for methanol oxidation [18].

However, several studies have reported on the dissolution of the transition metals in the alloy catalysts upon exposure to acids, although some of the alloys have been found to exhibit a higher electrocatalytic activity than pure metals [19,20]. Wieckowski et al. reported that the cobalt metal in Pt_3Co alloy catalyst dissolved in acidic media, whereas it was stable in alkaline media [21]. The alkaline condition has many advantages [22,23]. The kinetics of both oxygen reduction and methanol oxidation reactions are more favorable in alkaline media than in acidic media. Therefore, a non-Pt catalyst can be used in alkaline media. In addition, it seems possible to suppress the methanol crossover in direct alkaline methanol fuel cell [22], because the movement of hydroxide ions proceeds in the direction opposite to the movement of fuel crossover through the membrane, i.e., the direction of hydroxide ion movement is from cathode to anode. Thus, the management of water would be easy to perform in this system.

We have attempted to synthesize non-Pt catalysts using ultrasonic irradiation, in view of the known fact that the ultrasonic

* Corresponding author. Tel.: +81 3 5286 3202; fax: +81 3 3205 2074.
E-mail addresses: grass@moegi.waseda.jp (J. Kim), momma@waseda.jp (T. Momma), osakatets@waseda.jp (T. Osaka).

0378-7753/$ – see front matter © 2009 Elsevier B.V. All rights reserved.
doi:10.1016/j.jpowsour.2008.12.109

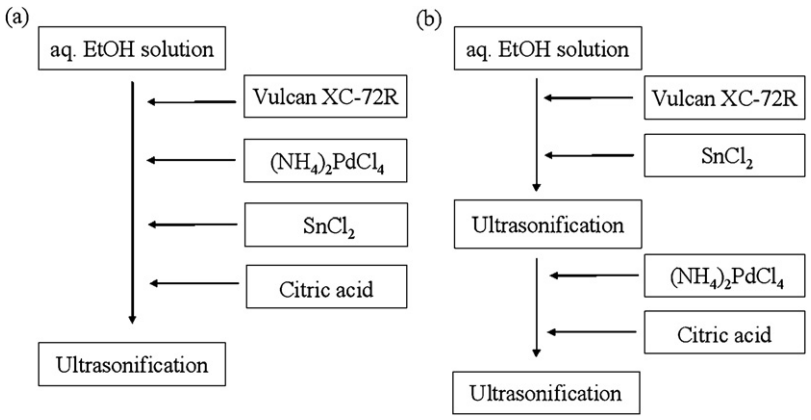

Fig. 1. Schematic diagrams for the preparation of carbon-supported Pd-Sn catalysts by (a) one-step ultrasonification (method 1) and (b) sequential reduction (method 2) ($Pd(NH_4)_2Cl_4$ = 0.0267 g, $SnCl_2$ = 0.016 g, citric acid = 10 mM, 10% ethanol).

reduction method generates noble metal nanoparticles with a much smaller size, a larger surface area, and a narrower size distribution than those prepared by other methods [24]. This method was expected to simplify the synthesis of bimetal nanoparticles with a specific structure such as the core-shell structure. Because this method does not use a reducing agent, no process for its removal is needed. For these reasons, the ultrasonic reduction method is expected to be a promising method of catalyst preparation for the fuel cell. In our previous studies, Pd-based nanoparticles were prepared under ultrasonic irradiation, and their activities toward the ORR have been evaluated in alkaline solution by using ITO electrodes modified with Pd-based nanoparticles. Pd-Sn nanoparticles prepared under ultrasonic irradiation showed a better ORR activity than Pt and Pd nanoparticles in alkaline media in the absence of methanol. Moreover, the Pd-Sn nanoparticles showed a higher ORR activity than Pt in the presence of 1 M methanol [25].

In this work, we investigated the possibility of utilizing ultrasonic irradiation for the preparation of carbon-supported metal catalyst by incorporating supporting carbon particles in the synthesis solution, and we demonstrated the potentiality of carbon-supported Pd-Sn catalyst as the oxygen reduction catalyst in alkaline media. We established a one-pot method for synthesizing Pd-Sn/C catalyst under ultrasonic irradiation and evaluated its electrocatalytic activity for oxygen reduction in alkaline media.

2. Experimental

2.1. Preparation of Pd/C and Pd-Sn/C catalysts

To prepare Pd-Sn/C catalyst, Vulcan XC-72R (Cabot Corp.) was used as a carbon support. Pd/C catalyst was prepared in the absence of Sn for comparison. Fig. 1 illustrates the procedure of synthesizing Pd-Sn/C catalyst. Method 1 uses one-step ultrasonification, while method 2 uses two-step ultrasonification for sequential reduction, in which the sources of the two metals are added separately into the synthesizing solution. For method 1, 0.08 g of Vulcan XC-72R was added with constant stirring into an aqueous 10 vol% ethanol solution and prepared by dissolving metal salts (0.0267 g of ammonium tetrachloropalladate and 0.016 g of tin chloride) and 10 mM citric acid as the stabilizing agent. This mixture was then irradiated by ultrasound. For method 2, Vulcan XC-72R was added with constant stirring into an aqueous ethanol solution prepared by dissolving tin chloride and citric acid as the stabilizing agent. After ultrasonification, an ammonium tetrachloropalladate solution was added into the irradiated solution. This solution was subjected to the second sonication process.

Ultrasonic irradiation was performed with a collimated 20 kHz beam from a ceramic transducer with a titanium amplifying horn (13 mmØ, Branson Sonofier 450D) directly immersed in the solution and operated with an input power of 42 W cm^{-2} for 2 h. The horn was vertically positioned 3 cm above the cell bottom. The power of ultrasound was determined by adiabatic measurement of the temperature rise of sonicated water. Temperature of the solution was kept constant in an ice bath during sonolysis.

All catalyst samples were washed with a large amount of H_2O and dried at 50 °C overnight.

2.2. Characterization of Pd/C and Pd-Sn/C catalysts

The shape and size of the Pd/C and Pd-Sn/C catalysts were observed using transmission electron microscopy (TEM, JEM-1011 operated at 100 kV). Specimens for TEM examination were prepared by placing a drop of Pd/C or Pd-Sn/C catalyst, dispersed in ethanol onto a carbon-coated copper grid, followed by natural evaporation of the solvent at room temperature. The metal loading of the catalysts was determined by inductively coupled plasma - optical emission spectrometer (ICP-OES). A CHN analyzer (Flash EA 1112) was used to determine the amount of carbon in the synthesized catalysts. The stabilizer remaining in the catalysts was determined by thermogravimetric analysis (TGA). The electronic structure of the catalysts was evaluated by X-ray photoelectron spectroscopy (XPS, JPS-9010TR) with Mg Kα radiation. The electron binding energy of the XPS was referred to the C1 s peak at 284.5 eV. XPS intensities were calculated by integrating peak areas after background subtraction. The X-ray diffraction (XRD) measurements were carried out on a RINT-TTRIII (Rigaku Co., Japan) using Cu Kα radiation (λ = 0.154 nm), which was operated at 50 kV and 100 mA. The 2θ angular regions between 20° and 85° were explored at a scan rate of 2° min^{-1}.

Electrocatalytic activities of the prepared catalysts for oxygen reduction were investigated in an oxygen saturated alkaline solution using a three-electrode electrochemical cell. The counter electrode was a platinum coil, and the reference electrode an Ag/AgCl. The working electrode was fabricated by casting a catalyst ink onto a glassy carbon electrode (10 mm in diameter). The ink was prepared by dispersing 5 mg of catalyst into 40 vol% ethanol. Linear sweep voltammetry (LSV) and rotating disk electrode (RDE) measurements were performed in 0.5 M KOH at a scan rate of 10 mV s^{-1}. All electrochemical measurements were carried out at room temperature. All electrode potentials measured by an Ag/AgCl reference electrode were converted to a reversible hydrogen electrode scale (RHE).

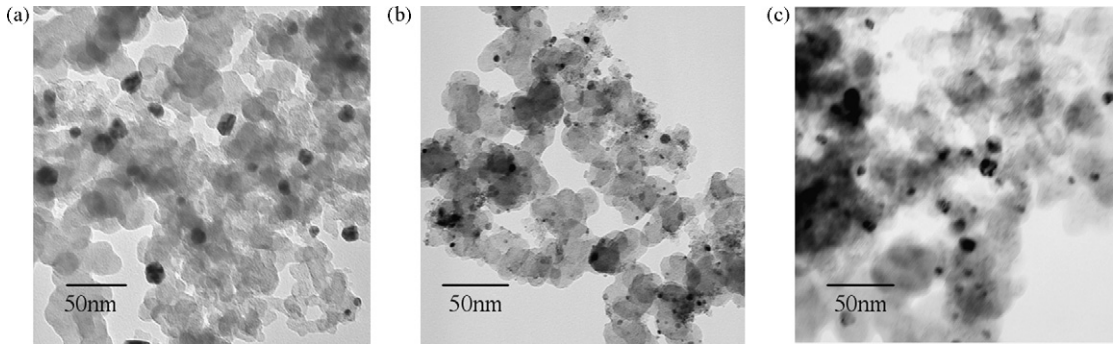

Fig. 2. TEM micrographs of (a) Pd/C catalyst, (b) Pd-Sn/C catalyst prepared by one-step ultrasonification (method 1), and (c) Pd-Sn/C prepared by sequential reduction (method 2) ($Pd(NH_4)_2Cl_4$ = 0.0267 g, $SnCl_2$ = 0.016 g, citric acid = 10 mM, 10% ethanol solution).

3. Results and discussion

3.1. Characterization of Pd/C and Pd-Sn/C catalysts

TEM images of Pd/C and Pd-Sn/C catalysts are shown in Fig. 2. From the images, metallic particles were confirmed to be precipitated on the surface of carbon. The particles of Pd/C catalyst was about 15 nm in average diameter (Fig. 2a). On the other hand, the Pd-Sn/C catalyst prepared by method 1 (Fig. 2b) and method 2 (Fig. 2c) had average diameter of about 3–5 and 5–10 nm, respectively, though some large aggregates were observed. It is clearly seen that Pd-Sn/C catalyst are smaller in particle size compared with the Pd/C catalyst. This implies that the catalyst size is decreased by the alloy formation of palladium with tin.

The metal loading of catalysts was measured by ICP. The metal loadings of Pd-Sn/C catalysts prepared by method 1 and method 2 were approximately the same, 11.8 wt% and 12.1 wt%, respectively, while Pd content was large than Sn content. The high Pd content can be explained by the fact that Pd is easier to reduce than Sn because the standard oxidation/reduction potential of $Pd(NH_4)_2Cl_4$ is 0.64 V, and that of $SnCl_2$ is −0.14 V [26]. However, catalysts prepared by the two methods had different Pd to Sn ratios. The Pd to Sn ratio of Pd-Sn/C catalysts prepared by method 1 was about 2.5, while that prepared by method 2 was about 1.7. That is, the Pd-Sn/C catalyst prepared by method 2 contained a larger amount of Sn than that prepared by method 1. The reason for this difference can be attributed to the difference in preparation processes. Pd and Sn metals should be deposited on carbon simultaneously in method 1, whereas in method 2 stepwise reduction of Pd and Sn metal ions to respective metals takes place on carbon, i.e., Sn ions are reduced before Pd ions by the first ultrasonification. This is believed to be the reason why the catalyst prepared by method 2 with the stepwise reduction had a larger Sn content than that prepared by method 1. However, the metal contents, especially those of tin, in these catalysts cannot be explained only by the fact that ultrasonification procedure was used. The Pd-Sn/C catalysts by each method were prepared varying ultrasonification time. The Pd-Sn/C catalysts prepared by the two methods showed different trends of Sn loading in proportion to ultrasonification time. Tin content decreased in the catalyst prepared by method 1, while that in the catalyst prepared by method 2 increased in proportion to the ultrasonification time. These results imply that the two methods proceed by different deposition mechanisms.

The stabilizer contents of the catalysts were determined by TGA. TGA curves of the catalysts are shown Fig. 3. Pd/C and Pd-Sn/C catalysts exhibited a weight loss in the vicinity of 150 °C, corresponding to the decomposition of citric acid. The TGA curves indicate that citric acid used as the stabilizer remained by the amount corresponding to about 2–4% in Pd/C and Pd-Sn/C catalysts. The Pd-Sn/C catalyst exhibited a larger weight loss than that of Pd/C catalyst. In addition, the catalysts showed different contents of residual citric acid depending on the preparation method. These results imply that the content of residual citric acid in carbon-supported catalysts influences the composition of catalysts, especially the tin content.

To investigate the effect of the remaining citric acid, we prepared Pd-Sn/C catalysts in the presence and in the absence of citric acid. Pd-Sn/C catalysts prepared in presence of citric acid exhibit high electrocatalytic activity for ORR because the citric acid improves the dispersion of catalysts on carbon, even though they have about 2–4% of citric acid. The improved electrocatalytic activity can be expected by removing the remaining citric acid in catalysts. However, the decrease of electrocatalytic activity is also anticipated because an increase of the particle size is indispensable during the heat treatment to remove the citric acid. Accordingly, we discussed the experimental results about catalyst without the heat treatment in this study.

Fig. 4 shows XRD patterns of the as-prepared Pd/C and Pd-Sn/C catalysts. The Pd/C catalyst showed fcc peaks of Pd [27]. The Pd-Sn/C catalyst prepared by method 1 also showed a typical fcc pattern with a slight positive shift in diffraction angles with respect to those of Pd/C catalyst. This indicates that the lattice of Pd is contracted due to partial displacement of Pd by Sn. This result is supported by the small size of Pd-Sn/C observed by TEM. However, the Pd-Sn/C catalyst prepared by method 2 did not show minor peaks corresponding to the fcc structure, although the broad major Pd (111) peak was observed. This result is attributed to incomplete phase

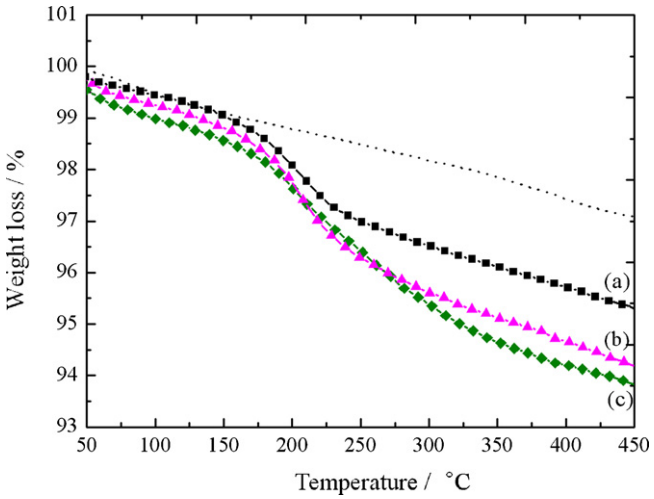

Fig. 3. TGA curves for as-prepared (a) Pd/C catalyst, (b) Pd-Sn/C catalyst prepared by one-step ultrasonification (method 1), and (c) Pd-Sn/C catalyst prepared by sequential reduction (method 2) ($Pd(NH_4)_2Cl_4$ = 0.0267 g, $SnCl_2$ = 0.016 g, citric acid = 10 mM, 10% ethanol) (dot line is a TGA curve for Pd/C catalyst prepared in absence of citric acid).

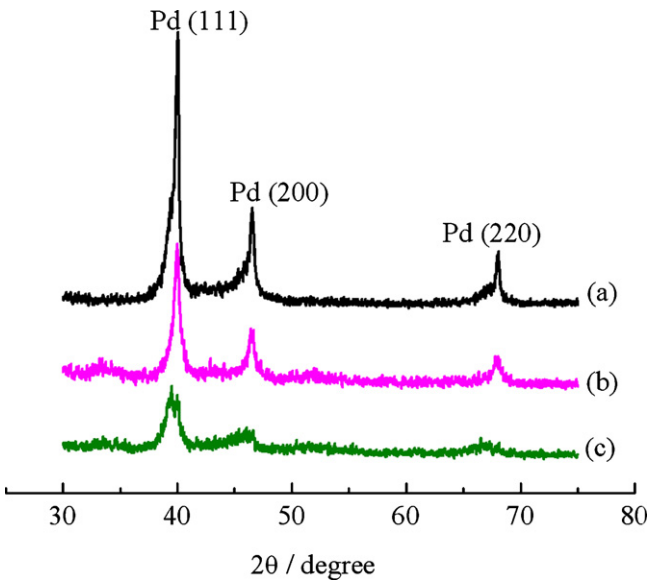

Fig. 4. XRD patterns for as-prepared (a) Pd/C catalyst, (b) Pd-Sn/C catalyst prepared by one-step ultrasonification (method 1), and (c) Pd-Sn/C catalyst prepared by sequential reduction (method 2) ($Pd(NH_4)_2Cl_4$ = 0.0267 g, $SnCl_2$ = 0.016 g, citric acid = 10 mM, 10% ethanol).

development because the sample was not thermally treated. XRD patterns of Pd-Sn/C electrocatalysts also showed peaks corresponding to tin oxides. This implies that a part of tin exists in the form of oxide, while the remainder of Sn forms an alloy with Pd [28].

The electronic structure of the surface of Pd/C and Pd-Sn/C catalysts was evaluated by X-ray photoelectron spectroscopy (Fig. 5). The Pd 3d levels of Pd/C and Pd-Sn/C catalysts show those of metallic palladium (340.5 eV (3d3/2) and 335.2 eV (3d5/2)) and palladium oxide (342.4 eV (3d3/2) and 337.1 eV (3d5/2)) [29,30]. Pd in Pd/C and Pd-Sn/C catalysts are in the forms of metal and oxide, though a larger portion of Pd exists in the metallic form. This result does not agree with the previous result that the Pd in the Pd-Sn nanoparticles was mostly in the metallic state [25]. It is known that electrons are transferred from metal microdeposits to carbon in a carbon-supported metal–catalyst system [31]. Contour et al. reported that the specific metal–support interaction is through electron transfer from platinum clusters to oxygen atoms of the surface of the support in the carbon-supported platinum PEMFC catalyst [32]. It could be explained that Pd oxide in carbon-supported catalysts is caused by interaction of Pd with oxygen atoms on the carbon surface. In addition, the Sn 3d level of Pd-Sn nanoparticles exhibited the binding energy of 486.7 eV (3d5/2), which is due to Sn oxide. The composition of Pd-Sn/C catalyst derived by using the XPS and ICP methods is summarized in Table 1. Both methods showed that the Pd-Sn/C catalysts prepared by method 1 contained a large amount of Pd than Sn. However, the calculated surface atomic ratios by XPS measurement showed that the Pd-Sn/C catalyst prepared by method 2 contained a larger amount of Sn than Pd. That result is contrary to the ICP result. This result indicates that the Pd-Sn/C catalyst prepared by method

Table 1
Atomic ratio of palladium to tin in Pd-Sn/C catalyst calculated by XPS and ICP methods (method 1 is one-step ultrasonification and method 2 is two-step ultrasonification).

	XPS			ICP		
	Pd	Sn	Pd/Sn	Pd	Sn	Pd/Sn
Method 1	56.7	43.3	1.31	71.7	28.3	2.53
Method 2	30.6	69.4	0.44	60.2	39.8	1.68
Pd	100	–	–	100	–	–

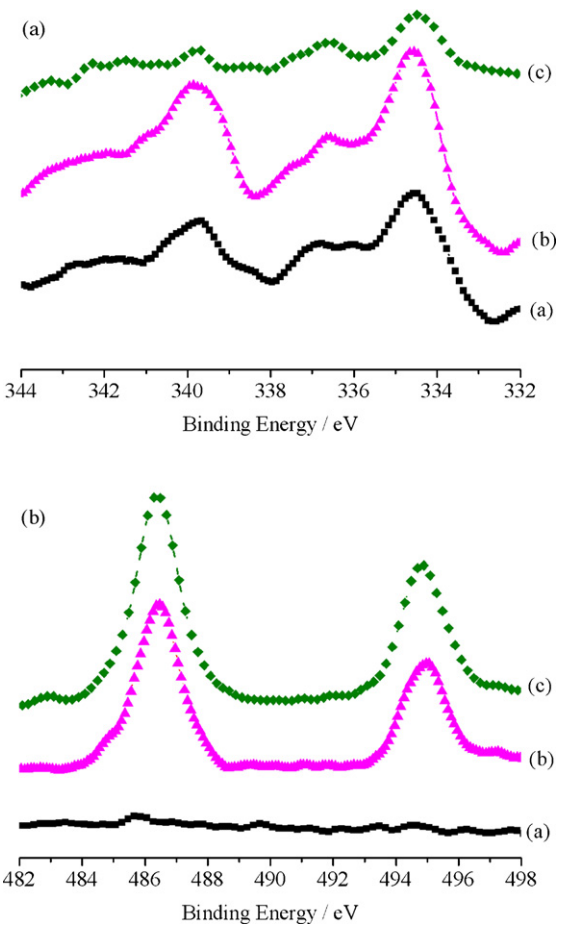

Fig. 5. XPS spectra of (a) Pd 3d level and (b) Sn 3d level of Pd/C catalyst (■)) and Pd-Sn/C catalysts. The latter catalysts were prepared by (b) one-step ultrasonification (method 1, ▲) and (c) sequential reduction (method 2, ♦) ($Pd(NH_4)_2Cl_4$ = 0.0267 g, $SnCl_2$ = 0.016 g, citric acid = 10 mM, 10% ethanol).

2 has a larger tin content on the surface than in the bulk. Kan et al. reported that Au/Pd bimetallic nanoparticles prepared by successive method have structure in which less reductive Pd atom exist on the Au [33], which is agreed with our results. Sn ions reduce to Sn particles during the first ultrasonification. During the second irradiation, the reduction of Pd ions to Pd atoms and the displacement of Sn atoms occur. As the irradiating time increases, the sonochemical reduction of Sn ions begins to dominate because most Pd ions are reduced. It has been reported that the reducing radicals do not disperse in solution at low concentration, but diffuse onto the formed Pd nanoparticles and polarize cathodically (double-layer-charging) [34]. Then, the Sn ions around Pd nanoparticles were reduced by the reducing radicals or the accumulated electrons on the surface of Pd. In addition, the parts of post-reduced Sn atoms form the alloy with Pd. In addition, Roman-Martinez et al. reported that Pt-Sn/C catalysts have a high surface atomic ratio of Sn to Pt because of the segregation of the second metal [35]. It is likely that the Pd-Sn/C catalyst also has a high surface atomic ratio of Sn to Pd.

3.2. Electrocatalytic activities of Pd/C and Pd-Sn/C catalysts

Electrocatalytic activities of the prepared catalysts for oxygen reduction were investigated in oxygen-saturated 0.5 M KOH. Fig. 6 shows linear scan voltammograms of Pd/C and Pd-Sn/C catalysts prepared by the two methods. All LSV curves show two peaks at about 0.8 V and 0.65 V vs. RHE, which are diffusion-controlled as the peak currents were found to be proportioned to the square root

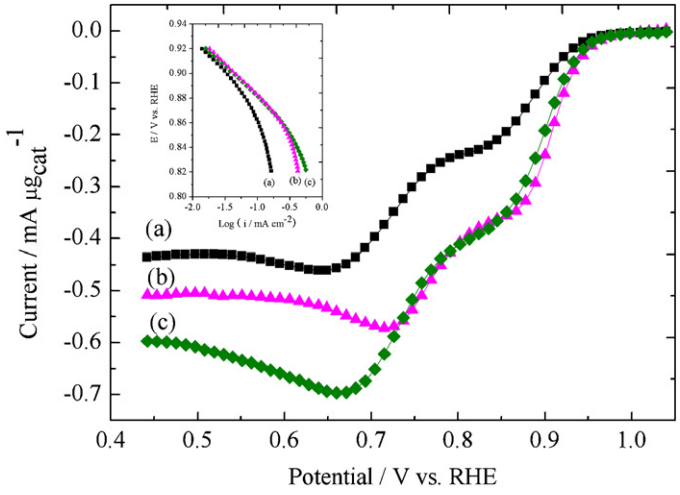

Fig. 6. Linear scan voltammograms for the as-prepared (a) Pd/C, and Pd-Sn/C catalysts prepared by (b) one-step ultrasonification (method 1) and (c) sequential reduction (method 2) in oxygen-saturated 0.5 M KOH (scan rate: 10 mV s^{-1}) (inset: Tafel plots for ORR on (a) Pd/C and Pd-Sn/C catalysts prepared by (b) method 1 and (c) by method 2, scan rate: 1 mV s^{-1}).

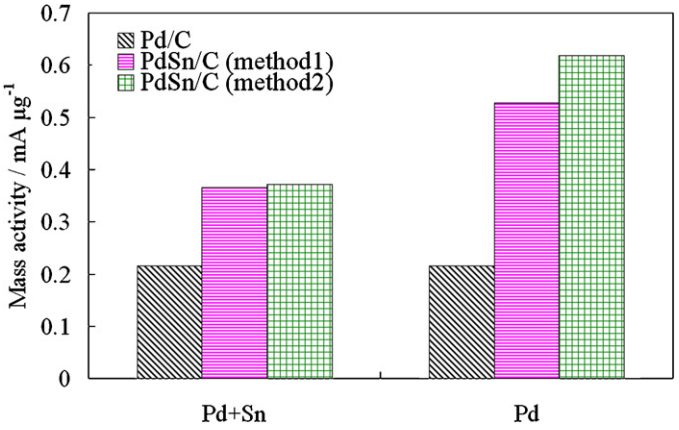

Fig. 7. Total metal (Pd + Sn) and Pd mass activities of Pd/C, and Pd-Sn/C catalysts prepared by one-step ultrasonification (method 1) and sequential reduction (method 2) for the ORR expressed in terms of mA g^{-1} at 0.8 V vs. RHE (−0.2 V vs. Ag/AgCl).

of scan rate. To assign the peaks, we evaluated the electrocatalytic activity of Pd-Sn nanoparticles, which were not supported on carbon, for ORR. Their oxygen reduction peak is observed at about 0.8 V vs. RHE (−0.2 V vs. Ag/AgCl). The numbers of electron transferred (n) for ORR calculated from rotating disk electrode experiments for Pd-Sn nanoparticles is 3.94. It indicates that oxygen reduction reaction at Pd-Sn nanoparticles mostly proceeds through the four-electron pathway. From these results, the peaks at about 0.8 V vs. RHE (−0.2 V vs. Ag/AgCl) are thought as the oxygen reduction peak on Pd-Sn catalyst. We also confirmed that the peak in vicinity of about 0.65 V vs. RHE (−0.35 V vs. Ag/AgCl) is the peak corresponding to oxygen reduction reaction on carbon surface from the electrochemical measurement using carbon black. Ticianelli et al. reported that the peroxide mechanism is operative at the carbon substrate, and that the four-electron reaction takes place at the platinum in alkaline media [36]. They reported that the four-electron mechanism predominates at the catalyst with more than 20% of platinum on carbon. Our results apparently indicate that oxygen reduction occurred both on the catalyst and on the carbon substrate, because the metal loading on carbon is less than about 15%.

The LSV curves for the Pd-Sn/C catalyst show a larger current of oxygen reduction and a more positive onset potential than for the Pd/C catalyst, meaning that the Pd-Sn/C catalyst has a higher ORR activity than the Pd/C catalyst in alkaline media. These results indicate that the addition of Sn enhances the oxygen reduction reaction on Pd. Onset potential of Pd-Sn/C catalysts exhibits about 0.9 V vs. RHE is similar to that of Pt/C catalysts and is more positive than that of Ag/C catalysts, which were reported by Coutanceau et al. [37]. This implies that the Pd-Sn/C catalyst prepared by using ultrasonic irradiation can be expected as a promising ORR catalyst in alkaline media. Fig. 7 shows the total metal (Pd and Sn) and Pd mass activity of the prepared catalysts expressed in terms of mA g^{-1} at 0.80 V vs. RHE (−0.2 V vs. Ag/AgCl) in 0.5 M KOH. The Pd mass activity of Pd-Sn/C is about 2.4 and 2.9 times greater, for the catalysts prepared by method1 and 2, respectively, than that of Pd/C catalyst. It is thought that a small particle size and an electronic stabilization of the alloying element in the alloy leaded to the enhancement of catalytic activity due to a synergic effect [38].

Two Tafel slopes were also observed for all electrocatalysts investigated in this study. The results are in agreement with the literature [18,39]. The catalytic mechanism for ORR at the Pd-Sn/C catalyst is likely to be similar to that at the Pd/C catalyst. The low and high Tafel slopes were −59 and −122 mV decade^{-1}, respectively, for the Pd/C catalyst. The Tafel slopes of the Pd-Sn/C prepared by method 1 and method 2 are −51 and −103 mV decade^{-1} and −48 and −110 mV decade^{-1}, respectively. The Tafel slopes of the Pd-Sn/C

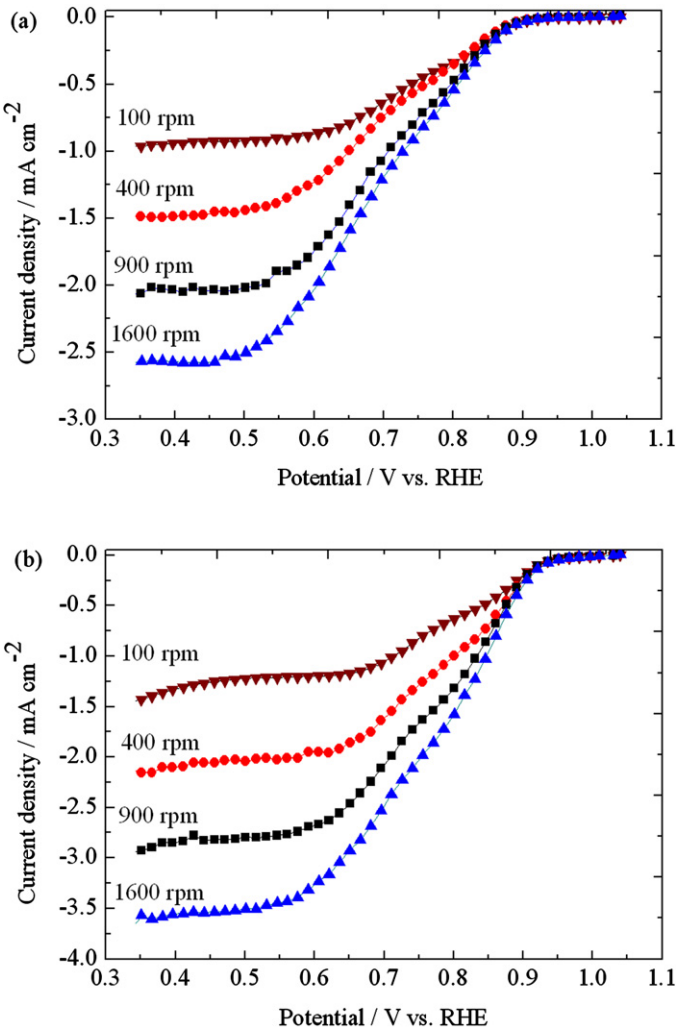

Fig. 8. Linear potential scan curves of (a) Pd/C and (b) Pd-Sn/C catalysts prepared by method 2 recorded at rotating disk electrodes in O_2 saturated 0.5 M KOH at various rotation rates (scan rate: 10 mV s^{-1}).

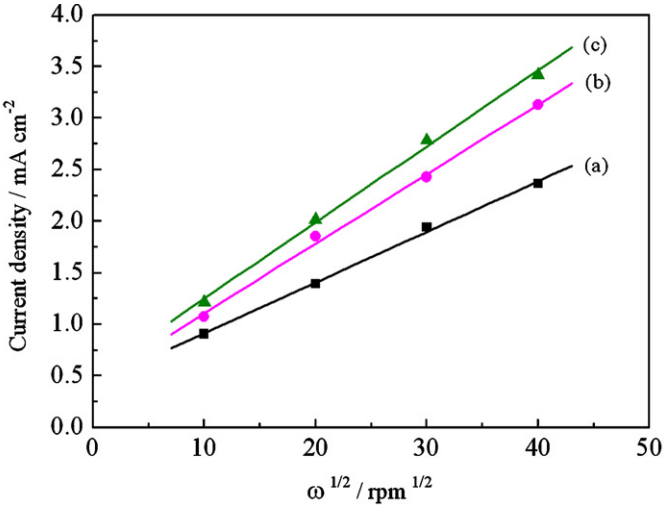

Fig. 9. Levich plots for the ORR on (a) Pd/C and (b and c) Pd-Sn/C catalysts. Pd-Sn/C catalysts were prepared by (b) one-step ultrasonification (method 1) and (c) sequential reduction (method 2) in oxygen-saturated 0.5 M KOH; scan rate: 10 mV s^{-1}, Current was measured at 0.5 V vs. RHE (−0.5 V vs. Ag/AgCl).

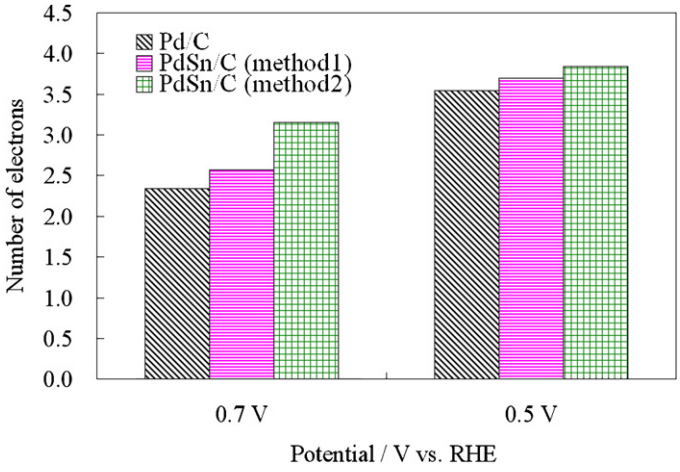

Fig. 10. Electron transfer numbers (n) of ORR on Pd/C and Pd-Sn/C catalysts prepared by method 1 and method 2. The n numbers were calculated from the slope of Koutechy–Levich plots at 0.7 V and 0.5 V vs. RHE (−0.3 V and −0.5 V vs. Ag/AgCl), respectively.

catalyst are smaller than those of the Pd/C catalyst. This finding indicates that the Pd-Sn/C catalyst has a higher electrocatalytic activity for ORR than the Pd/C catalyst, because the addition of Sn affects the formation of Pd oxide.

Fig. 8 shows LSV curves for oxygen reduction at disk electrodes recorded at various rates of rotation. The Pd-Sn/C catalyst prepared by method 2 (Fig. 8b) showed a larger limiting current density than the Pd/C catalyst in spite of the same catalyst loading. This result indicates that at the Pd-Sn/C catalyst, the ORR reaction involves a larger number of electrons than that at the Pd/C catalyst. Levich plots of the prepared Pd/C and Pd-Sn/C catalysts are shown in Fig. 9. I_d values obtained at 0.5 V vs. RHE were used in Fig. 9. It is seen that the Levich plot of Pd/C and Pd-Sn/C catalysts yielded straight lines with different slopes. This result implies that Sn content affects the number of electrons involved in the ORR at the catalysts.

$$I^{-1} = {I_d}^{-1} + {I_K}^{-1} \quad (1)$$

$$I_d = 0.620\, nFA\, Do^{2/3} \omega^{1/2} \upsilon^{-1/6} Co_2^* \quad (2)$$

$$I_K = nFAK\Gamma_{cat} Co_2^* \quad (3)$$

where I_d (A) is the diffusion-limited current for the electrode reaction of reactive species, and I_K (A) is the kinetic current for the reaction of reactive species at the electrode surface. n (mol^{-1}) is the number of electrons transferred per O_2 molecule, F is the Faraday constant (96,500 C mol^{-1}), A (cm^2) is the electrode area (0.785 cm^2), Do (cm^2 s^{-1}) is the oxygen diffusion coefficient in 0.5 mol L^{-1} KOH (= 1.68×10^{-5} cm^2 s^{-1}), $($ (s^{-1}) is the rotation rate, υ (cm^2 s^{-1}) is the kinematic viscosity of 0.5 mol L^{-1} KOH (0.01064 cm^2 s^{-1}), Co_2^* (mol cm^{-3}) is the concentration of O_2 in 0.5 mol L^{-1} KOH at 25 °C (= 1.031×10^{-6} mol L^{-1}) [40]. K (M^{-1} s^{-1}) is the rate constant for O_2 reduction, and Γ_{cat} (mol cm^{-2}) is the quantity of catalyst on the surface of the electrode.

Fig. 10 shows the numbers of electron transferred (n) for ORR calculated from the slope of the Koutechy–Levich plots for all catalysts. The n value for ORR at Pd/C for ORR is 3.5, while the n value of the Pd-Sn/C catalysts prepared by method 1 and method 2 are 3.7 and 3.8, respectively. The Pd-Sn/C catalyst showed a larger number of electrons for ORR than the Pd/C catalyst. That is, the four-electron reaction of ORR is more favorable on Pd-Sn/C catalyst than on Pd/C catalyst. Especially, the n values for the Pd/C catalyst and the Pd-Sn/C catalyst in the low potential region, e.g. 0.7 V vs. RHE, are 2.3 and 3.2, respectively. As already mentioned, the two-electron reaction of ORR at the carbon substrate is more favorable at low metal loadings on carbon. However, the addition of Sn to Pd/C catalyst makes the four-electron reaction more favorable than the two-electron reaction at the carbon surface.

Based on these results, it can be stated that the ORR activity of Pd-Sn/C catalyst is enhanced its increased surface area resulting from its small particle size, and that the addition of Sn increase the number of electrons involved in the ORR reaction.

4. Conclusions

The Pd-Sn/C catalyst was successfully synthesized by ultrasonic irradiation of the solution containing metal ions and carbon support, and its electrocatalytic activity was evaluated in alkaline media. The Pd-Sn/C catalyst has better ORR activity than the Pd/C catalyst in alkaline media. The enhanced ORR activity is attributed to the effect of small particle size and the electronic interaction of Pd and Sn. In addition, the addition of Sn promotes the four-electron reaction of ORR on the catalyst surface more than two-electron reaction on the carbon surface at low metal loading catalyst. Although the oxygen reduction reaction on the catalyst metal was not the total reaction in our experiments, a complete $4e^-$ reaction of ORR can be achieved by preparing a high metal loading catalyst with heat treatment. Based on these results, the Pd-Sn/C catalyst prepared by using ultrasonic irradiation is expected as a promising ORR catalyst in alkaline media.

Acknowledgements

This work was supported partly by the Global COE Program "Center for Practical Chemical Wisdom", the Encouraging Development Strategic Research Center's Program "Establishment of Consolidated Research Center's Institute for Advanced Science and Medical Care", and partly by the Grant-in-Aid for Specially Promoted Research "Establishment of Electrochemical Device Engineering" from the Ministry of Education, Culture, Sports, Science and Technology (MEXT)", Japan.

References

[1] S.C. Thomas, X.M. Ren, S. Gottesfeld, P. Zelenay, Electrochim. Acta 47 (2002) 3741–3748.
[2] A.K. Shukla, P.A. Christensen, A.J. Dickinson, A. Hamnett, J. Power Sources 76 (1998) 54–59.

[3] J.G. Liu, T.S. Zhao, R. Chen, C.W. Wong, Electrochem. Commun. 7 (2005) 288–294.
[4] L. Zhang, J. Zhang, D.P. Wilkinson, H. Wang, J. Power Sources 156 (2006) 171–182.
[5] H.A. Gasteiger, S.S. Kocha, B. Sompalli, F.T. Wagner, Appl. Catal. B: Environmental 56 (2005) 9–35.
[6] U.B. Demirci, J. Power Sources 173 (2007) 11–18.
[7] B. Wang, J. Power Sources 152 (2005) 1–15.
[8] N.R. Rivera, H.N. Castillo, A. Soto-Guzman, B.O. Solorza-Feria, Int. J. Hydrogen Energy 27 (2002) 457–460.
[9] O. Savadogo, K. Lee, K. Oishi, S. Mitsushima, N. Kamiya, K. Ota, Electrochem. Commun. 6 (2004) 105–109.
[10] J.M. Zen, R. Manoharan, J.B. Goodenough, J. Appl. Electrochem. 22 (1992) 140–150.
[11] N. Alonso Vante, H. Tributsch, O. Solorza-Feria, Electrochim. Acta 40 (1995) 567–576.
[12] S.S. Ozenler, F. Kadırgan, J. Power Sources 154 (2006) 364–369.
[13] G. Faubert, G. Lalande, R. Cote, D. Guay, J.P. Dodelet, L.T. Weng, P. Bertrand, G. Denes, Electrochim. Acta 41 (1996) 1689–1701.
[14] F. Jaouen, S. Marcotte, J.P. Dodelet, G. Lindbergh, J. Phys. Chem. B 107 (2003) 1376–1386.
[15] J.L. Fernandez, V. Raghuveer, A. Manthiram, A.J. Bard, J. Am. Chem. Soc. 127 (2005) 13100–13101.
[16] V. Raghuveer, A. Manthiram, A.J. Bard, J. Phys. Chem. B 109 (2005) 22909–22912.
[17] J.L. Fernandez, D. Walsh, A.J. Bard, J. Am. Chem. Soc. 127 (2005) 357–365.
[18] K. Lee, O. Savadogo, A. Ishihara, S. Mitsushima, N. Kamiya, K. Ota, J. Electrochem. Soc. 153 (2006) A20–A24.
[19] V.R. Stamenkovic, B.S. Mun, K.J.J. Mayrhofer, P.N. Ross, N.M. Markovic, J. Am. Chem. Soc. 128 (2006) 8813–8819.
[20] M. Wakisaka, S. Mitsui, Y. Hirose, K. Kawashima, H. Uchida, M. Watanabe, J. Phys. Chem. B 110 (2006) 23489–23496.
[21] H.T. Duong, M.A. Rigsby, W. Zhou, A. Wieckowski, J. Phys. Chem. C 111 (2007) 13460–13465.
[22] J.R. Varcoe, R.C.T. Slade, Fuel Cells 5 (2005) 187–200.
[23] R.C.T. Slade, S. Robert, J.R. Varcoe, Solid State Ionics 176 (2005) 585–597.
[24] K. Vindgopal, Y. He, M. Ashokkumar, F. Grizer, J. Phys. Chem. B 110 (2006) 3849–3852.
[25] J. Kim, J.E. Park, T. Momma, T. Osaka, ECS Trans. 11 (31) (2008) 51–60.
[26] A.J. Bard, Encyclopedia of Electrochemistry of the Elements, M. Dekker, vol. VI, IV, New York, 1976.
[27] M.H. Shao, K. Sasaki, R.R. Adzic, J. Am. Chem. Soc. 128 (2006) 3526–3527.
[28] Y. Guo, Y. Zang, M. Huang, Electrochim. Acta 53 (2008) 3102–3108.
[29] H. Yang, N. Alonso-Vante, C. Lamy, D.L. Akins, J. Electrochem. Soc. 152 (2005) A704–A709.
[30] C.D. Wagner, W.M. Riggs, L.E. Davis, J.F. Moulder, G.E. Muilenberg, Handbook of X-Ray Photoelectron Spectroscopy, Perkin-Elmer Corporation Physical Electronics Division, Eden Prairie, MN, 1979, p. 82.
[31] V.S. Bogotski, A.M. Snudkin, Electrochim. Acta 29 (1984) 757–765.
[32] J.J. Escard, C. Leclerc, J.P. Contour, Catalysis 29 (1973) 31–39.
[33] C. Kan, W. Cai, C. Li, L. Zhang, H. Hofmeister, J. Phys. D: Appl. Phys. 36 (2003) 1609–1614.
[34] P. Mulvaney, M. Giersig, A. Henglein, J. Phys. Chem. 96 (1992) 10419–10424.
[35] M.C. Roman-Martınez, J.A. Macia-Agullo, I.M. Julieta-Vilella, D. Cazorla-Amoros, H. Yamashita, J. Phys. Chem. C 111 (2007) 4710–4716.
[36] F.H.B. Lima, E.A. Ticianelli, Electrochim. Acta 49 (2004) 4091–4099.
[37] L. Demarconnay, C. Coutanceau, J.-M. Léger, Electrochim. Acta 49 (2004) 4513–4521.
[38] M.M. Jaksic, Electrochim. Acta 45 (2000) 4085–4099.
[39] A. Bolzan, M.E. Martins, A.J. Arvia, J. Electroanal. Chem. 207 (1986) 279–292.
[40] C.F. Zinola, A.M.C. Luna, W.E. Triaca, A.J. Arvia, J. Appl. Electrochem. 24 (1994) 531–541.